FERMILAB-CONF-77-164-E

COHERENT DISSOCIATION OF NEUTRONS*

(This note is based on a report presented by T. Ferbel at the VIIth International Conference on High Energy Physics and Nuclear Structure at Zurich (1977), and is a preliminary version of an analysis carried out mainly by Dr. W. Mollet. Dr. Mollet died on August 14th in a climbing accident in the Adirondacks.)

W. Mollet, J. Biel, T. Ferbel#, P. Slattery
and D. Underwood

University of Rochester

B. Gobbi, L. Kenah, J. Rosen, R. Ruchti

Northwestern University

E. Bleser

Fermilab

D. Freytag

SLAC

Data are presented from Fermilab on the dissociation of neutrons into $p\pi^-$ systems using a variety of nuclear targets. The absorption of the $p\pi^-$ systems in nuclear matter and the production and decay characteristics of these systems are examined and compared with data on a hydrogen target. It is observed that production on nuclear targets is characterized by rather unusual features in decay angular distributions and in momentum transfers.

*Research supported by U.S. Energy Research and Development Administration. (under contract number EY-76-C-02-3065.000)

#I thank the National Science Foundation for providing travel funds for attending the Zurich Conference.

September 20, 1977

Coherent exclusive production channels have been used in the past to obtain total cross sections (σ^*) for the interaction of unstable systems with nucleons.[1] By studying the atomic-number (A) dependence of reactions such as:

$$n + A \rightarrow (p\pi^-) + A \tag{1}$$

$$p + A \rightarrow (p\pi^+\pi^-) + A \tag{2}$$

$$\pi^- + A \rightarrow (\pi^-\pi^+\pi^-) + A \tag{3}$$

it has been possible, with the aid of Glauber-type of scattering model, to extract σ^* values for different kinds of multihadron systems. In a recent article, Fäldt[2] indicated that models, such as the most favored Kolbig-Margolis[3] formulation, which ignore possible contributions of spin-flip terms to coherent production, may provide incorrect estimates of total cross sections for the interaction of these unstable systems with nucleons. In this note I will present experimental results which complement Fäldt's remarks, and suggest that large spin-flip type of contributions may, in fact, be present in certain kinematic regions of coherent production. Consequently, ignoring the presence of such terms may result in the extraction of rather meaningless values for σ^*. In addition, I will indicate that nuclear targets may be particularly sensitive to the details of mechanisms contributing to diffraction production.

The data I will discuss were obtained in our investigation of reaction (1) at Fermilab. General features of these data were presented earlier,[4] and a more recent work, detailing the extraction of σ^*, has been submitted for publication.[5]

Figures 1 and 2 reproduce some of the important features of reaction (1) as given in ref. (5). Figure 1(a) displays the differential cross section for reaction (1) on a copper target for the $p\pi^-$ mass (m)

interval $1.35 < m < 1.45$ GeV. The t' variable is equal to $(p_L\theta_L)^2$, where p_L and θ_L are the momentum and angle of the $p\pi^-$ system in the laboratory frame. The calculated Coulomb-dissociation contribution (Primakoff production) to reaction (1) is indicated in the graph. (Although the electromagnetic cross section peaks sharply at $t' \sim 4 \times 10^{-6}$ GeV^2, resolution substantially broadens that distribution.) The figure also shows the sum of the calculated Coulomb term and the nuclear diffraction component (using the Kolbig-Margolis Model), for different values of σ^*, superimposed on the data. The A-dependence of the cross section for the same mass interval as in (a) is given in Fig. 1(b). Again, the Coulomb and the nuclear-model calculations are shown for comparison with the data. (Several typical error bars are also indicated on the data points in Fig. 1.)

Figure 2 displays mass spectra for production on C, Al, Cu and Pb targets, for two intervals in t': $t' < 0.001$ GeV^2 in (a), where Coulomb production is important; and $0.005 < t' < 0.030$ GeV^2 in (b), where hadronic processes dominate. The cross section in Fig. 2(a), at smallest masses (in the $\Delta(1236)$ region), is approximately proportional to Z^2, where Z is the nuclear charge; while in Fig. 2(b), particularly at large masses, the cross section is only weakly dependent on target material. These are just the sort of features expected for the two coherent-production processes. (The shaded region in Fig. 2(b) shows the calculated contribution from Coulomb production in Pb. The width of the band indicates the uncertainty in the Primakoff calculation due to uncertainty in the photoproduction data for the reaction $\gamma n \to p\pi^-$ at low energies, which is used in calculating the electromagnetic component in reaction 1.) Finally, also displayed in Fig. 2(c), are the results of extracting σ^* from fits to the kind of data shown previously in Fig. 1(b). The values

of σ^* are substantially smaller than the known total cross sections of $\sim$40 mb for nucleon-nucleon scattering.

Now I wish to present new data on the decay angles of the $p\pi^-$ system in reaction (1). Figure 3 displays distributions of Gottfried-Jackson polar angle (θ_{GJ}) of the proton, as a function of m, for Cu and C data. Two very unusual features are apparent in the figure. First, is that at all mass values, there appears to exist a clear steep enhancement in the data at large negative $\cos\theta_{GJ}$. Second, is that the $\cos\theta_{GJ}$ distribution shifts to more positive values as the mass increases. (Although there seems to be a dip in some of the data near $\cos\theta_{GJ} \simeq 1$, the region of $\cos\theta_{GJ} > 0.9$ has both poor statistics and poor acceptance, particularly for large masses.) These features are similar to previous observations reported for reaction (1) at lower energies. In particular, the data of Mühlemann et al,[6] which are available only for $\cos\theta_{GJ} \gtrsim -0.2$, and the data of Vander Velde et al,[7] which are for $\cos\theta_{GJ} < 0.0$, are both in general agreement with our measurements in regions of mutual overlap. For comparison, data for reaction (1), on a hydrogen target,[8] are given in Fig. 4.

We showed in a previous publication[9] that the t' distribution for production on hydrogen was a strong function of $\cos\theta_{GJ}$. Of particular interest were the facts that for $\cos\theta_{GJ} > 0.9$ the t distribution appeared to display a minimum at t' = 0, and that for $\cos\theta_{GJ} < -0.9$ the t distribution was peaked at t' = 0, while for $|\cos\theta_{GJ}| < 0.3$ the t' spectrum was exceedingly steep, displaying a rather sharp minimum at $t' \simeq 0.2$ GeV^2 (this last effect was particularly dramatic for small m values). These results were compared to a Deck-like model, which was only partially successful in accommodating the data. The model was quite good (except for a factor of two in the overall normalization) in the region of phase space where the π-exchange graph of Fig. 5 was

dominant, namely, the region of $\cos\theta_{GJ} > 0.9$.

Figure 6 presents the previously published data on hydrogen[9] for convenient comparison with t' distributions on a Cu target for data with $1.165 < m < 1.550$ GeV, and $1.55 < m < 1.85$ GeV, in Fig. 7, and 8, respectively. It is clear that, ignoring the first several t' bins (dominantly Coulomb production), the shapes of these t' spectra are also strongly dependent on $\cos\theta_{GJ}$. In fact, the shapes in t for $t' \lesssim 0.01$ GeV^2 range from exp(-265 t') for data at $|\cos\theta_{GJ}| < 0.3$ in Fig. 7 to exp(-140 t') for data at $\cos\theta_{GJ} < -0.9$ in Fig. 8. After an initial, exceedingly steep, drop off for $t' \lesssim 0.003$ GeV^2 (similar to that expected for the Coulomb-production contribution shown in Fig. 1), the data for $\cos\theta_{GJ} > 0.9$ in Fig. 7 show only a weak fall off in t'. (The expected Coulomb contribution to data in Fig. 8 is substantially smaller than that in Fig. 7.) The weak t' dependence for data with small θ_{GJ} suggests that substantial helicity-flip terms contribute in this region of phase space. Figures 9 and 10 display results for Be and C targets (combined to improve statistics), which confirm the variation of the t' spectra in nuclei with changes in θ_{GJ}.

Several interesting implications emerge from the extraordinarily large variations observed in the slopes of the t' spectra (the shape of the elastic scattering distribution for protons on Cu[10] can be represented approximately as exp(-180 t)). First, is that extraction of σ^* through an averaging over such differing t distributions must certainly be suspect to some extent. Second, is that production on nuclear targets must be exceedingly sensitive to the details of the diffraction mechanism. In particular, the sharp rises observed in the t' distributions in hydrogen for $\cos\theta_{GJ} < -0.9$ and for $|\cos\theta_{GJ}| < 0.3$ are amplified and seen

just as clearly on nuclear targets, and the same is true for the weak t' dependence for $\cos\theta_{GJ} > 0.9$. Also, the rise in the cross section for $\cos\theta_{GJ} \lesssim -0.6$, which was not observed in the hydrogen data (recall that these data were only for $t > 0.02$ GeV^2), must, in the context of the Deck Model, reflect the dominance of the baryon-exchange contributions over π-exchange for very small t values.

To summarize, examining the trends of the data for reaction (1) as a function of t, it appears that, although production on nuclear targets may connect smoothly with production on hydrogen, there are nevertheless surprising features in the nuclear data which provide new challenges to models which attempt to describe the diffraction dissociation mechanism. In addition, it appears that substantial helicity-flip amplitudes may be present in certain regions of phase space and, consequently, as emphasized by Fäldt, ignoring such contributions altogether in extracting cross sections for scattering of unstable systems on nucleons, can often yield inconsistent and erroneous results.

References

1. See, for example, R. Edelstein et al, Phys. Rev. Letts. 38, 185 (1977) and W. Beusch et al, Physics Letts. 55B, (1975).

2. G. Fäldt, Proc. of Topical Meeting on High Energy Collisions at ICTP, Trieste (1976).

3. K. Kölbig and B. Margolis, Nucl. Phys. B6, 85 (1968).

4. T. Ferbel, Proc. of E.P.S. Int'l. Conf. on High Energy Physics Palermo (1975), Editrice Compositori, A. Zichichi, ed.

5. W. Mollet, J. Biel, T. Ferbel, P. Slattery, D. Underwood, B. Gobbi, L. Kenah, J. Rosen, R. Ruchti, E. Bleser and D. Freytag. Rochester/Northwestern/FNAL/SLAC Collaboration, University of Rochester Report UR-623 (1977), submitted to Phys. Rev. Letts. for publication.

6. P. Mühlemann et al, University of Rochester Report UR-631, submitted to Nucl. Phys. B. for publication (1977).

7. J. Vander Velde et al, Nucl. Phys. B45, 1 (1972).

8. J. Biel, Ph.D. Thesis, University of Rochester (1977).

9. J. Biel, et al, Physics Letts. 65B, 291 (1976).

10. H. R. Blieden et al, Phys. Rev. D11, 14 (1975).

Figure Captions

1. Differential cross section for reaction (1) on a Cu target for the $p\pi^-$ mass interval between 1.35 GeV and 1.45 GeV, and the atomic number dependence of the cross section for $t < 0.02$ GeV^2 are given in (a) and (b), respectively. Both graphs are for neutron-momenta between 200 and 260 GeV/c. The absolute prediction for the Coulomb contribution is shown both separately and combined with the nuclear-model expectations for different N*N total cross sections.

2. Mass dependence of the cross section for reaction (1) at small and at larger t values. The best-fit values extracted for the N*N total cross section are given in (c).

3. Distributions in the Gottfried-Jackson polar angles for Cu and C targets, presented as a function of mass, for $t < 0.05$ GeV^2. The data have large losses in acceptance for $\cos\theta_{GJ} > 0.9$, and consequently the results in that bin, particularly at large mass, have additional systematic uncertainty. (Several statistical error bars are shown on the acceptance-corrected angular distributions.)

4. Angular distribution in θ_{GJ} for hydrogen data, presented as a function of mass, for two intervals in t.

5. Diagrams which are thought to contribute to diffraction production in reaction (1).

6. Distributions in momentum transfer, as a function of mass and $\cos\theta_{GJ}$, for hydrogen data. The curves are predictions based on the graphs given in Fig. 5, but reduced by an arbitrary factor of $\sim$2 for comparison with the data.

7. Distributions in momentum transfer on a Cu target for three regions of $\cos\theta_{GJ}$. The data are for masses between 1.165 and 1.55 GeV and incident neutron momenta between 150 and 300 GeV/c.

8. Distributions in momentum transfer on a Cu target for three regions of cos θ_{GJ}. The data are for masses between 1.55 and 1.85 GeV and incident neutron momenta between 150 and 300 GeV/c.

9. Distributions in momentum transfer on a C target for three regions of cos θ_{GJ}. The data are for masses between 1.165 and 1.55 GeV and incident neutron momenta between 150 and 300 GeV/c.

10. Distributions in momentum transfer on a C target for three regions of cos θ_{GJ}. The data are for masses between 1.55 and 1.85 GeV and incident neutron momenta between 150 and 300 GeV/c.

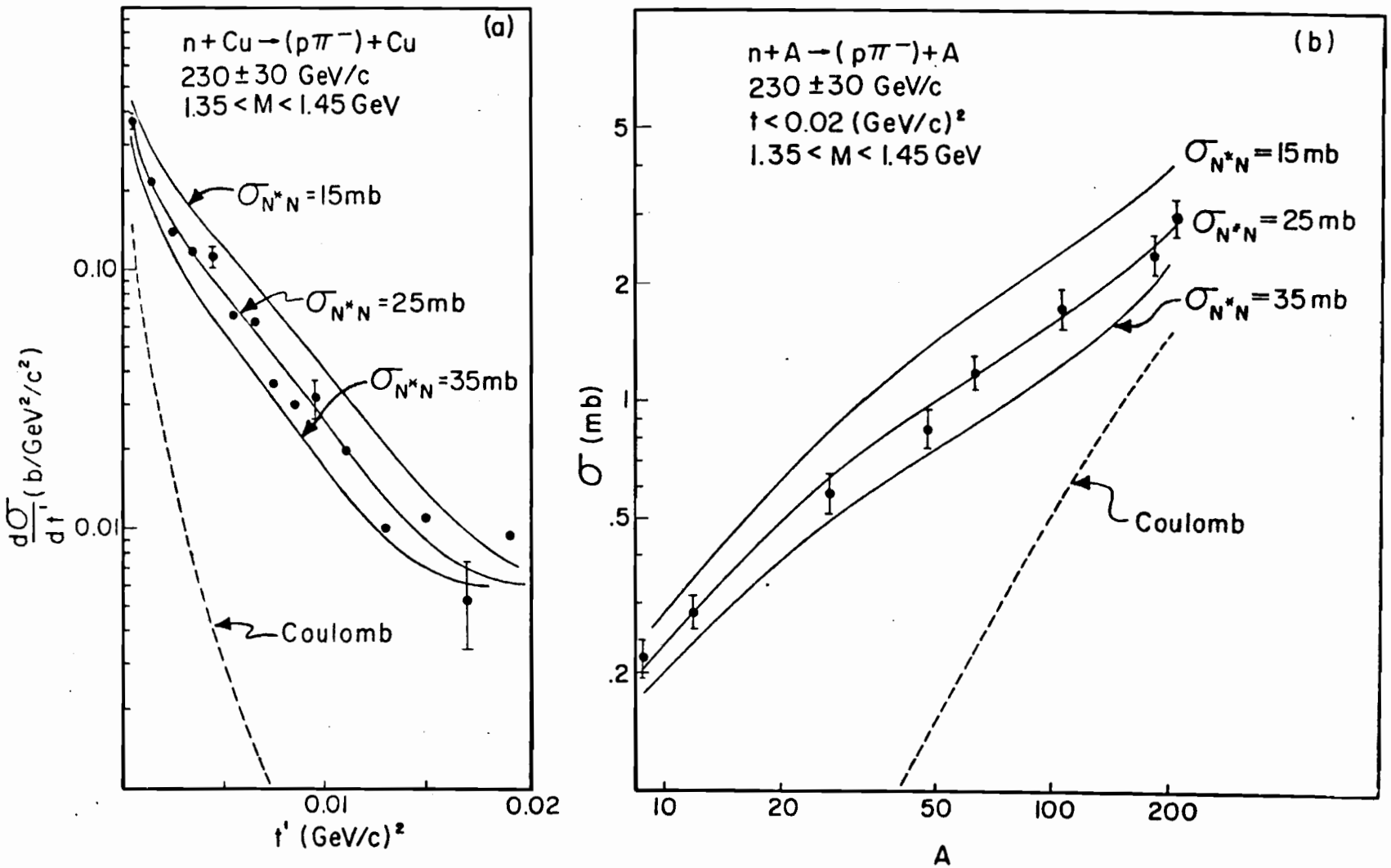
(a)
n + Cu → (pπ⁻) + Cu
230 ± 30 GeV/c
1.35 < M < 1.45 GeV
σ_N*N = 15mb
σ_N*N = 25mb
σ_N*N = 35mb
Coulomb
0.10
0.01
dσ/dt' (b/GeV²/c²)
0.01
0.02
t' (GeV/c)²
(b)
n + A → (pπ⁻) + A
230 ± 30 GeV/c
t < 0.02 (GeV/c)²
1.35 < M < 1.45 GeV
σ_N*N = 15mb
σ_N*N = 25mb
σ_N*N = 35mb
Coulomb
5
2
1
.5
.2
σ (mb)
10
20
50
100
200
A

1

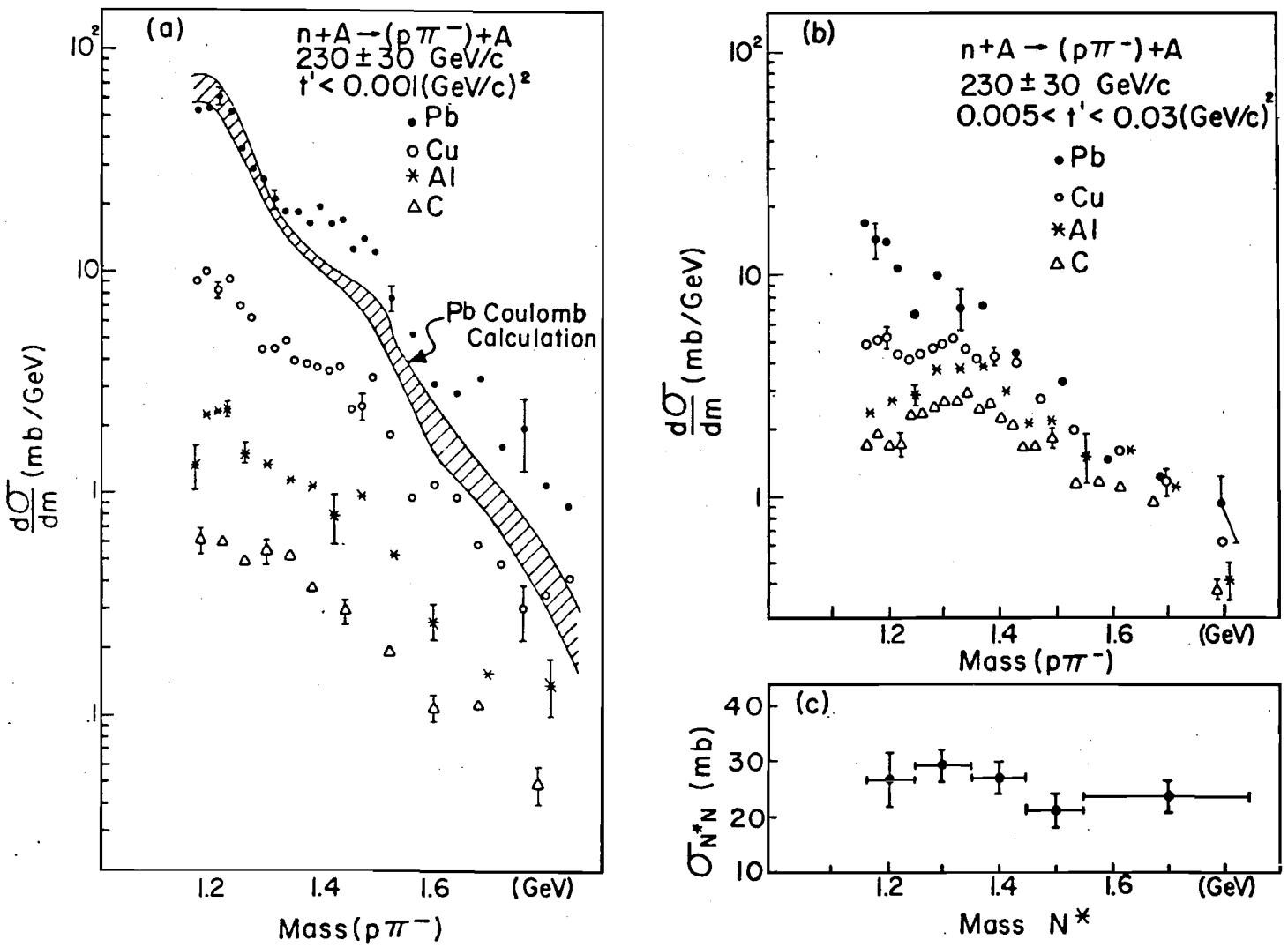
(a)
n+A→(pπ⁻)+A
230±30 GeV/c
t'< 0.001(GeV/c)²
• Pb
○ Cu
* Al
△ C
Pb Coulomb Calculation
dσ/dm (mb/GeV)
Mass (pπ⁻)
(GeV)
(b)
n+A → (pπ⁻)+A
230±30 GeV/c
0.005< t'< 0.03(GeV/c)²
• Pb
○ Cu
* Al
△ C
dσ/dm (mb/GeV)
Mass (pπ⁻)
(GeV)
(c)
σ_N*N (mb)
Mass N*
(GeV)

2

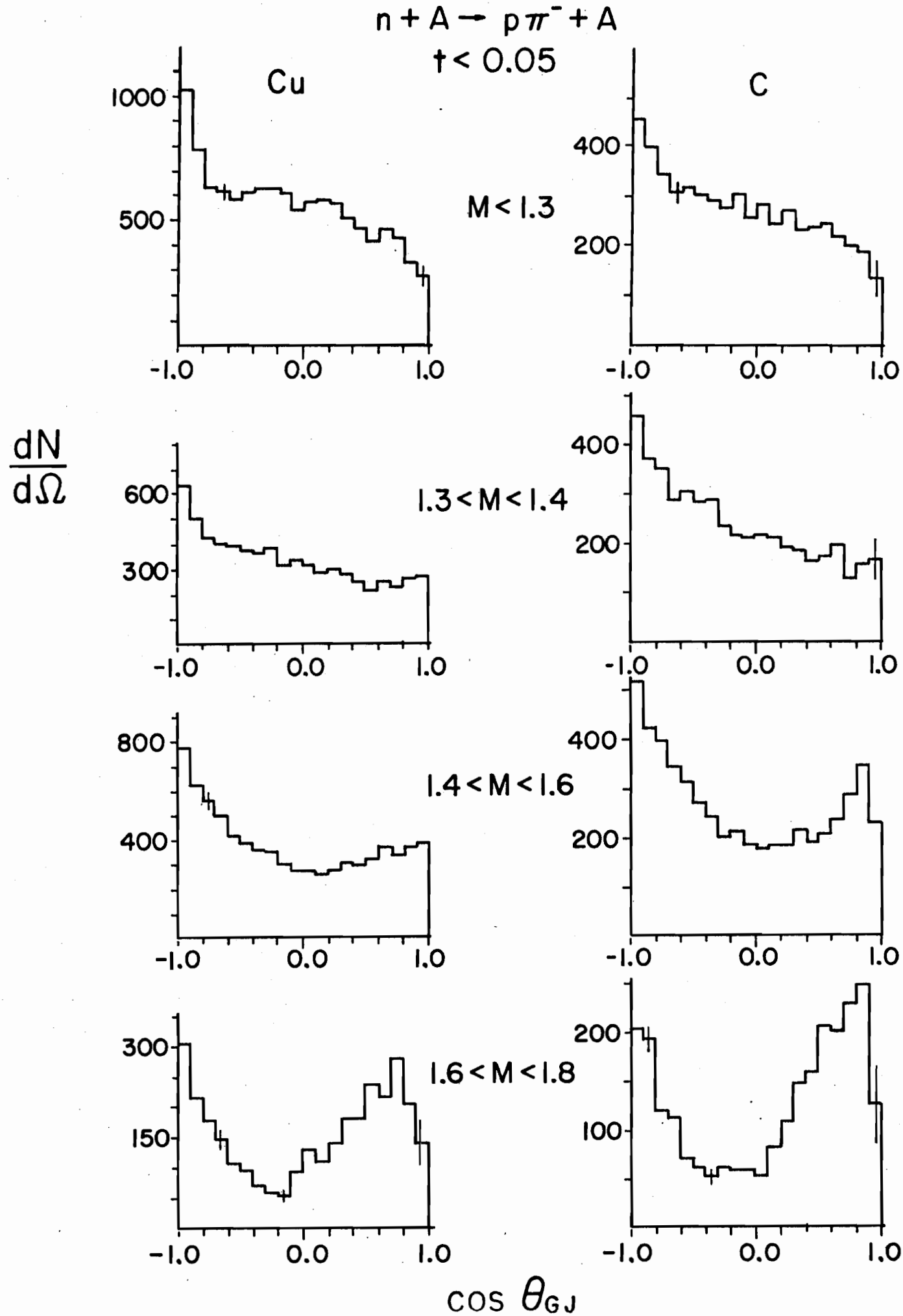
n + A → pπ⁻ + A
t < 0.05
Cu
C
M < 1.3
1.3 < M < 1.4
1.4 < M < 1.6
1.6 < M < 1.8
dN/dΩ
cos θGJ
1000
500
400
200
600
300
800
400
300
150
-1.0
0.0
1.0

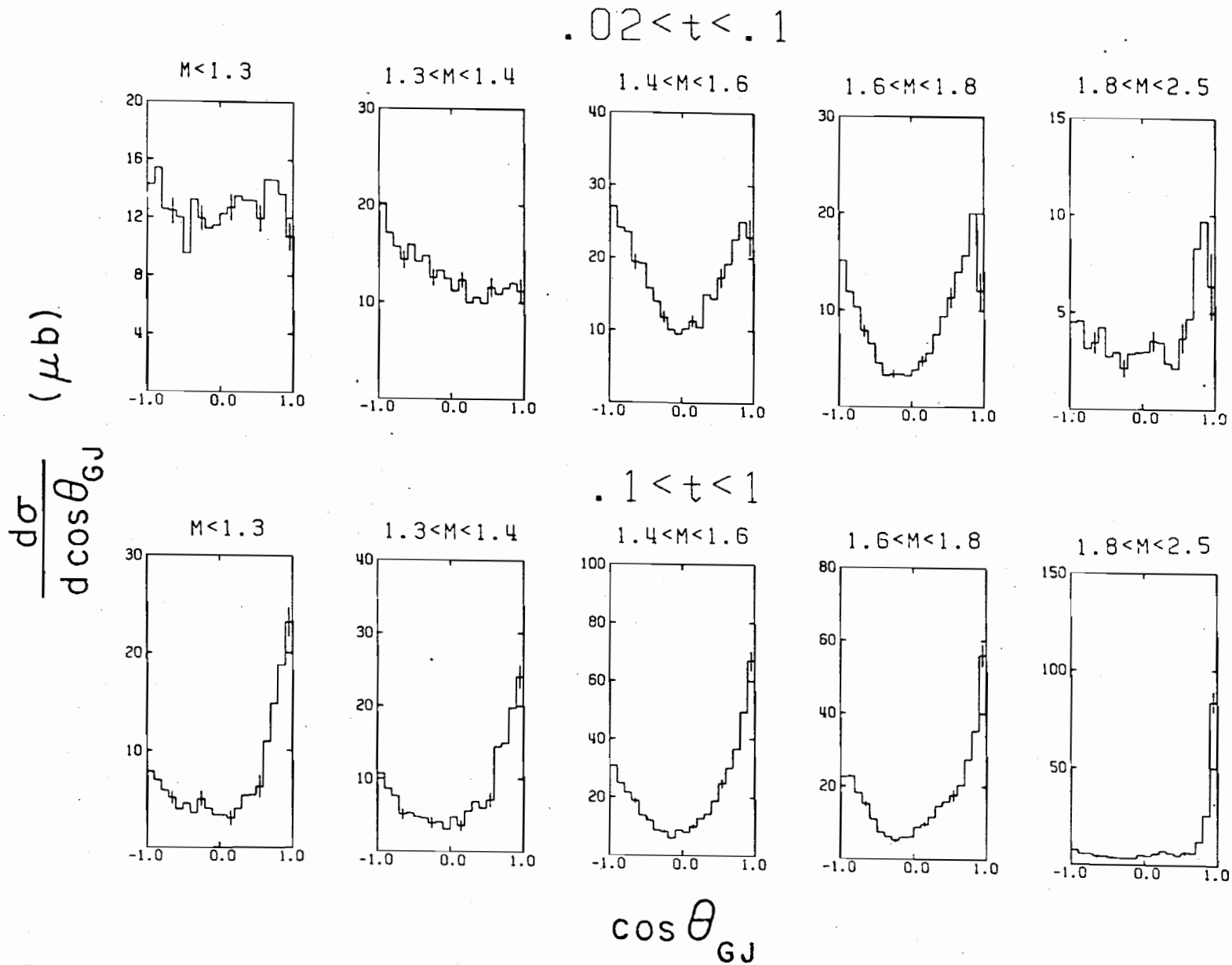
.02<t<.1
M<1.3
1.3<M<1.4
1.4<M<1.6
1.6<M<1.8
1.8<M<2.5
.1<t<1
M<1.3
1.3<M<1.4
1.4<M<1.6
1.6<M<1.8
1.8<M<2.5
$\frac{d\sigma}{d\cos\theta_{GJ}}$ (μb)
$\cos\theta_{GJ}$

4

(a) pion exchange Deck

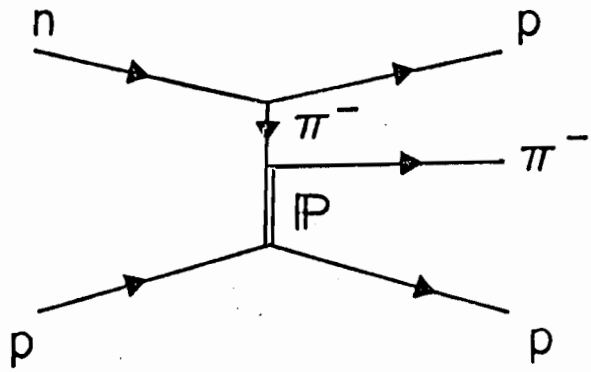

(b) proton exchange Deck

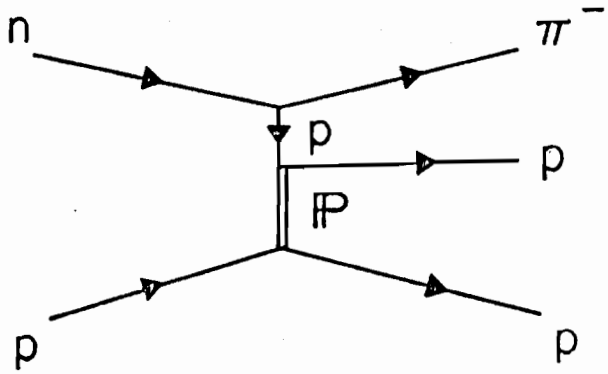

(c) direct production

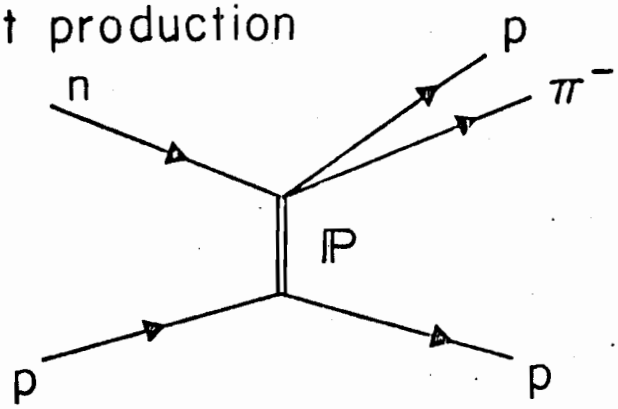

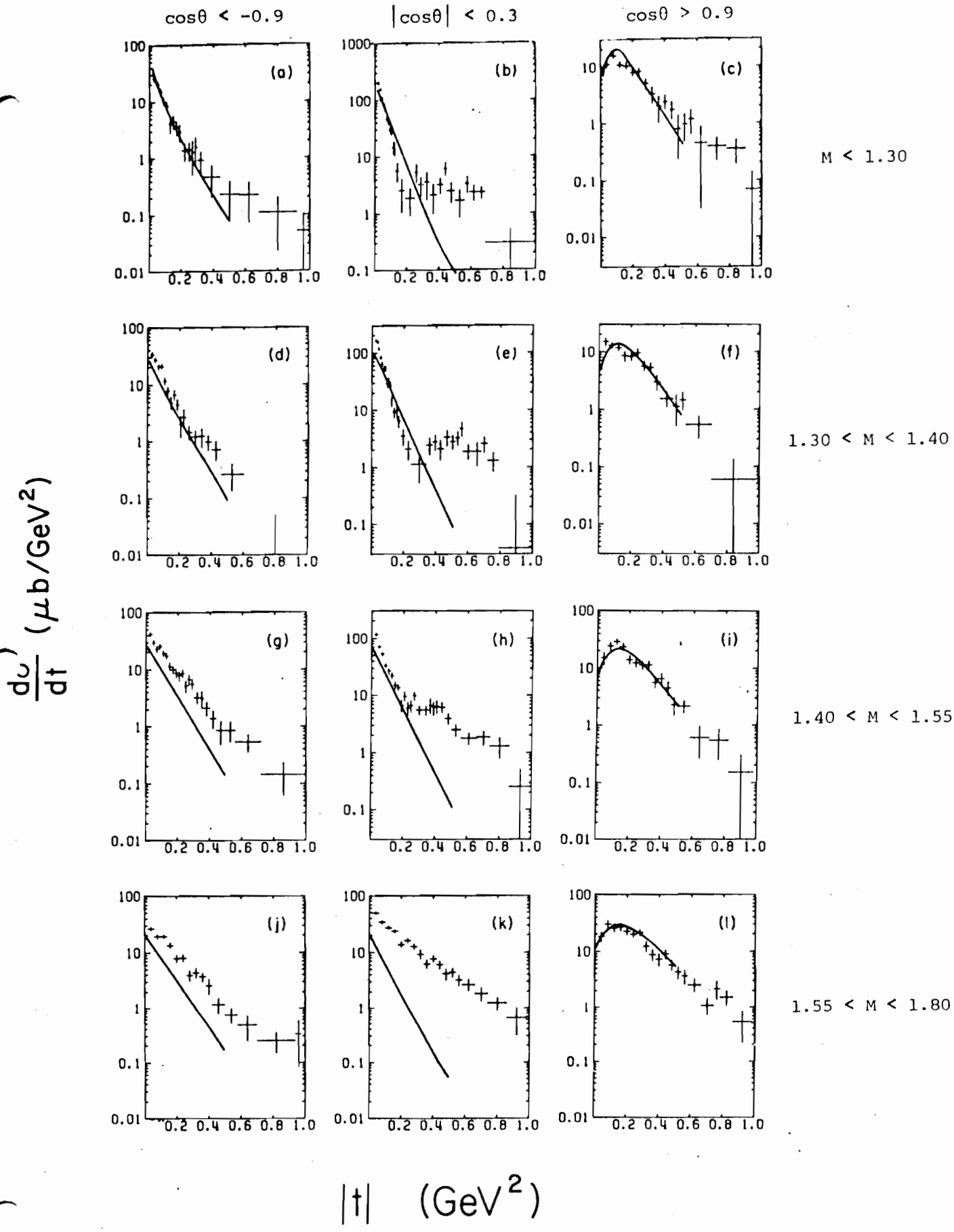
cosθ < -0.9
|cosθ| < 0.3
cosθ > 0.9
(a)
(b)
(c)
(d)
(e)
(f)
(g)
(h)
(i)
(j)
(k)
(l)
M < 1.30
1.30 < M < 1.40
1.40 < M < 1.55
1.55 < M < 1.80
dσ/dt (μb/GeV²)
|t| (GeV²)

Fig. 6

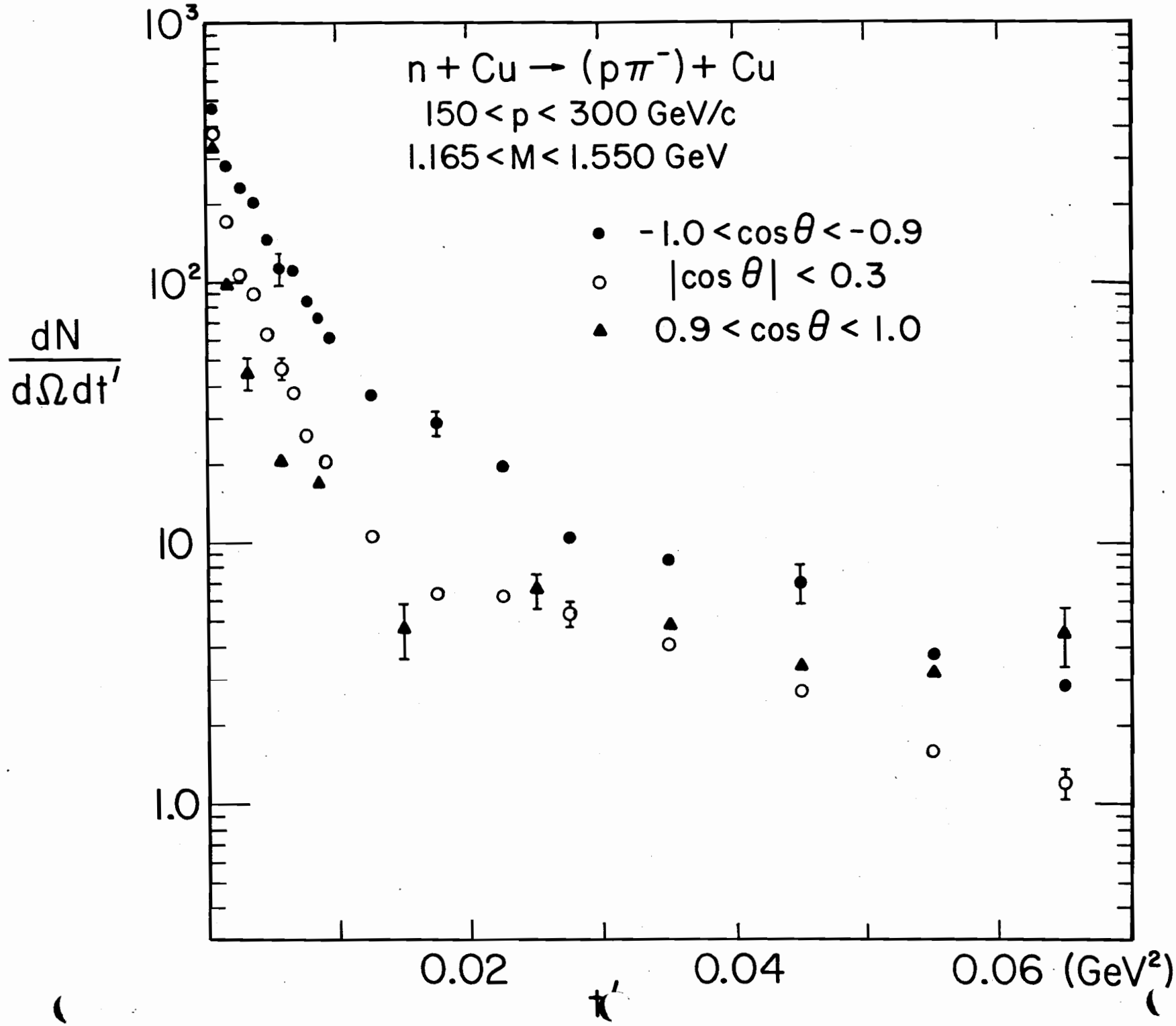
n + Cu → (pπ⁻) + Cu
150 < p < 300 GeV/c
1.165 < M < 1.550 GeV
-1.0 < cos θ < -0.9
|cos θ| < 0.3
0.9 < cos θ < 1.0
dN / dΩdt′
10³
10²
10
1.0
0.02
0.04
0.06 (GeV²)
t′

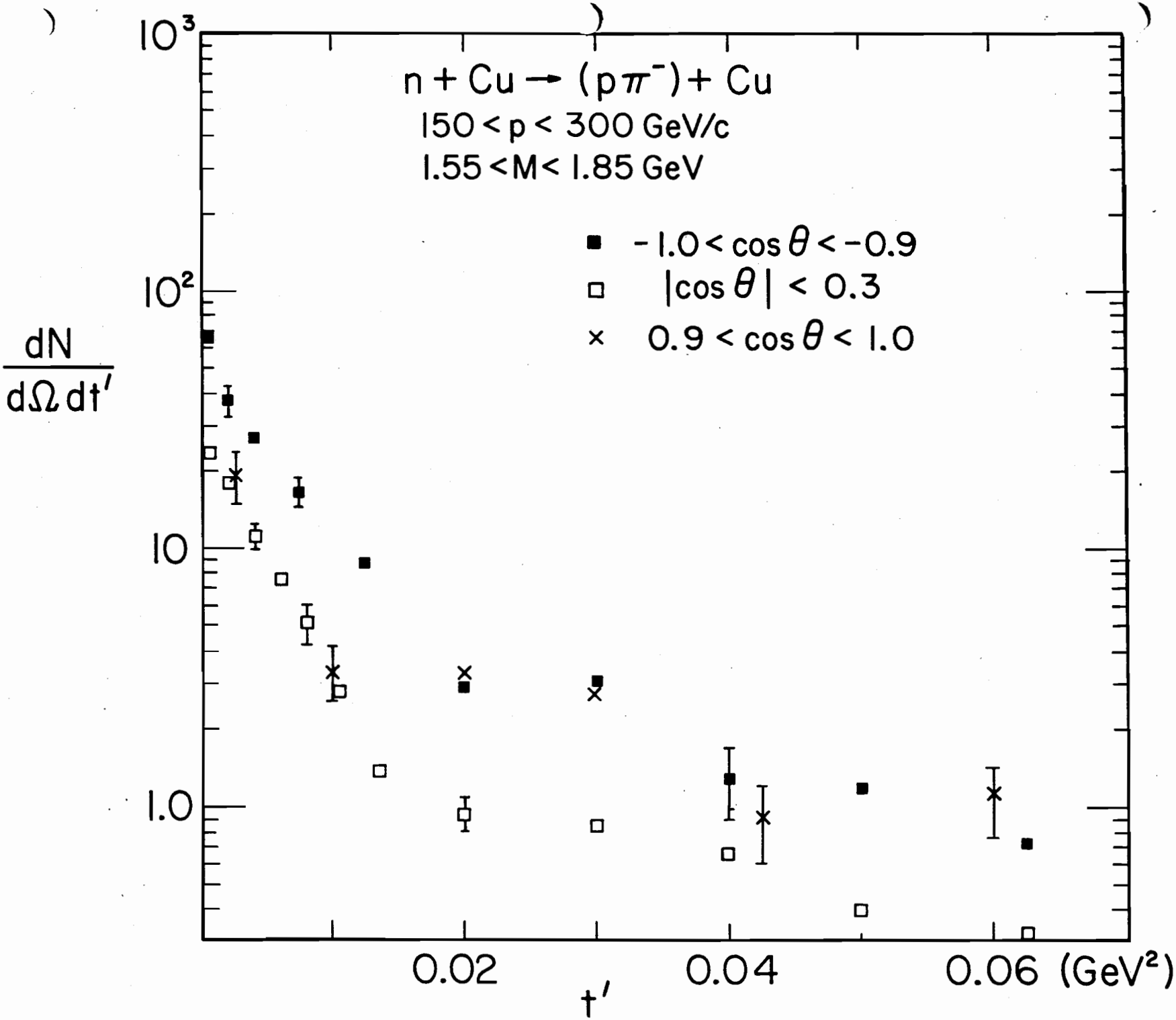
n + Cu → (pπ⁻) + Cu
150 < p < 300 GeV/c
1.55 < M < 1.85 GeV
-1.0 < cos θ < -0.9
|cos θ| < 0.3
0.9 < cos θ < 1.0
dN / dΩ dt′
10³
10²
10
1.0
0.02
0.04
0.06 (GeV²)
t′

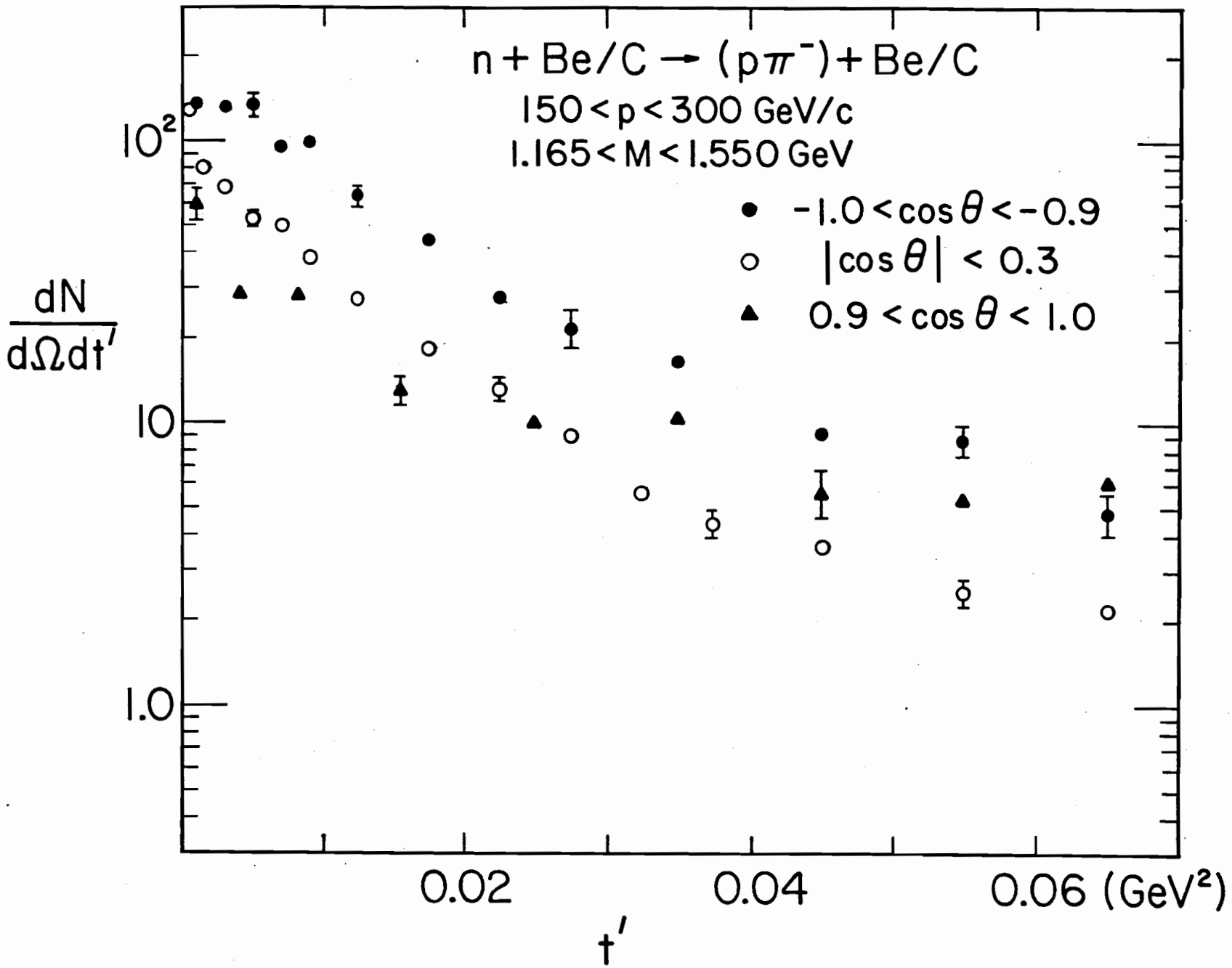
n + Be/C → (pπ⁻) + Be/C
150 < p < 300 GeV/c
1.165 < M < 1.550 GeV
-1.0 < cos θ < -0.9
|cos θ| < 0.3
0.9 < cos θ < 1.0
dN / dΩdt′
10²
10
1.0
0.02
0.04
0.06 (GeV²)
t′

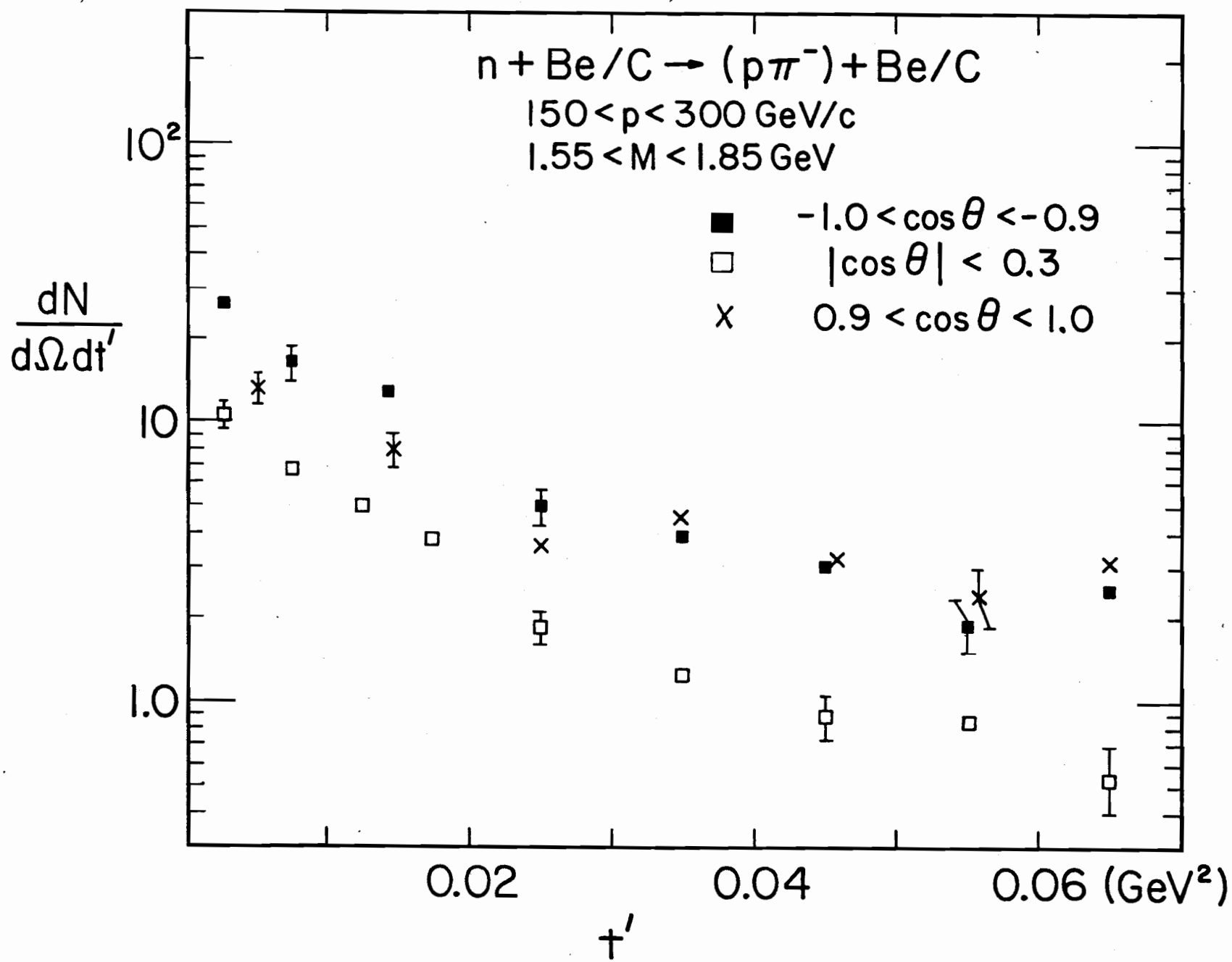
n + Be/C → (pπ⁻) + Be/C
150 < p < 300 GeV/c
1.55 < M < 1.85 GeV
-1.0 < cos θ < -0.9
|cos θ| < 0.3
0.9 < cos θ < 1.0
dN / dΩdt'
10²
10
1.0
0.02
0.04
0.06 (GeV²)
t'